# Dynamic switching enables efficient bacterial colonization in flow

Anerudh Kannan[a], Zhenbin Yang[b], Minyoung Kevin Kim[c], Howard A. Stone[d], and Albert Siryaporn[a,e,1]

[a]Department of Physics and Astronomy, University of California, Irvine, CA 92697; [b]Department of Physics, Princeton University, Princeton, NJ 08544; [c]Frick Laboratory, Department of Chemistry, Princeton University, Princeton, NJ 08544; [d]Department of Mechanical and Aerospace Engineering, Princeton University, Princeton, NJ 08544; and [e]Department of Molecular Biology and Biochemistry, University of California, Irvine, CA 92697

Edited by Curtis G. Callan, Jr., Princeton University, Princeton, NJ, and approved April 10, 2018 (received for review October 27, 2017)

**Bacteria colonize environments that contain networks of moving fluids, including digestive pathways, blood vasculature in animals, and the xylem and phloem networks in plants. In these flow networks, bacteria form distinct biofilm structures that have an important role in pathogenesis. The physical mechanisms that determine the spatial organization of bacteria in flow are not understood. Here, we show that the bacterium *P. aeruginosa* colonizes flow networks using a cyclical process that consists of surface attachment, upstream movement, detachment, movement with the bulk flow, and surface reattachment. This process, which we have termed dynamic switching, distributes bacterial subpopulations upstream and downstream in flow through two phases: movement on surfaces and cellular movement via the bulk. The model equations that describe dynamic switching are identical to those that describe dynamic instability, a process that enables microtubules in eukaryotic cells to search space efficiently to capture chromosomes. Our results show that dynamic switching enables bacteria to explore flow networks efficiently, which maximizes dispersal and colonization and establishes the organizational structure of biofilms. A number of eukaryotic and mammalian cells also exhibit movement in two phases in flow, which suggests that dynamic switching is a modality that enables efficient dispersal for a broad range of cell types.**

bacterial dispersal | bacterial mechanics | biofilm organization | colonization dynamics | *P. aeruginosa*

Spatial organization within a bacterial biofilm, which is a dense multicellular community of cells, is important for the survival of a bacterial population and for pathogenesis (1, 2). Biofilm organization is dictated by a number of factors, including the availability of nutrients, signaling molecules, and mechanical forces (1–9). For example, obligate aerobes develop biofilms at liquid–air interfaces in cultures (10) and form wrinkled structures in colonies to maximize oxygen absorption (11). In environments that contain moving fluids, the mechanisms responsible for large-scale biofilm organization are not understood but have important implications for host health, pathogenesis, and persistence. Bacterial biofilms form in the complex flow networks of human and animal blood and lymph circulatory systems, digestive and urinary tracts, the lung, in the fluidic networks of plants, and in the waterways of natural settings (1, 2). In healthcare settings, bacteria form biofilms in medical devices that contain flow, including stents, i.v. fluid lines, and catheters, presenting a serious challenge to healthcare professionals and the medical industry. In particular, the establishment of biofilms in flow can lead to the clogging of flow pathways (12–16), cutting off nutrients to vital locations. What are the mechanisms that dictate bacterial organization at the single-cell level and at large scales in these flow networks? Such mechanisms would appear to be important for predicting the outcomes of host colonization and pathogenesis, but are not understood.

*Pseudomonas aeruginosa* is an opportunistic bacterial pathogen that infects a broad range of organisms including humans, animals, plants, and fungi. In humans, *P. aeruginosa* infects areas that contain moving fluids, causing sepsis and pneumonia. Biofilm formation is important for *P. aeruginosa* infection mechanisms and is initiated by surface attachment, a critical step that also activates the expression of virulence factors (2, 17–22). Cells attach to surfaces through two modes: reversible or irreversible attachment (17–19, 23). Cells that attach irreversibly remain stationary on the surface, whereas those that attach reversibly can detach to the bulk, move on surfaces through twitching motility, or reattach to surfaces. The interaction of these attachment modes with shear stress generated by flow is not understood but is likely to play a significant role in shaping biofilm structure and organization. In addition, *P. aeruginosa* respond to flow by moving upstream. This process is due to the polar attachment of cells using type IV pili and the alignment of cells in the upstream direction by shear stress (24, 25). Type IV pili contribute to, but are not required for, surface attachment (26–28). The combined effects of upstream movement on surfaces, downstream movement in the bulk, and attachment dynamics in flow are unknown and likely contribute to the developmental organization of biofilms. The effects of these processes in complex flow networks are important in healthcare and infection settings but have not been characterized. In particular, no quantitative model exists to predict the outcomes of bacterial colonization in such networks.

Here, we investigate the temporal and spatial dynamics of *P. aeruginosa* in flow during the early stages of biofilm formation. We observe that *P. aeruginosa* performs continuous cycles of surface attachment, upstream surface migration, detachment, downstream advection with the bulk, and surface reattachment.

## Significance

**Bacteria colonize surfaces and form dense biofilm communities in natural and infection settings where flow is present. The physical mechanisms that give rise to the spatial organization of biofilms in flow are not understood. Here, we show that the bacterium *Pseudomonas aeruginosa* uses a process that we have termed dynamic switching to efficiently disperse throughout a flow network and maximize spatial colonization. This process dictates the spatial organization of cells during the transition from individual cells to multicellular biofilm communities. Thus, dynamic switching establishes the initial organizational structure of biofilms. The motion of many eukaryotic cell types can be described by dynamic switching, which suggests a general role of this process in a broad range of cellular systems.**

Author contributions: A.K., Z.Y., M.K.K., H.A.S., and A.S. designed research; A.K., Z.Y., M.K.K., and A.S. performed research; A.K. and A.S. analyzed data; and A.K., H.A.S., and A.S. wrote the paper.

The authors declare no conflict of interest.

This article is a PNAS Direct Submission.



Data deposition: Simulation code and experimental data has been deposited at GitHub at https://github.com/asirya/DynamicSwitching.

[1]To whom correspondence should be addressed. Email: asirya@uci.edu.

This article contains supporting information online at www.pnas.org/lookup/suppl/doi:10.1073/pnas.1718813115/-/DCSupplemental.

Published online May 7, 2018.

This cyclical process, which we have termed dynamic switching, maximizes the spatial distribution of cells in flow. The equations that describe dynamic switching are identical to those that describe the dynamic instability of microtubules during the search and capture of chromosomes during cell division (29). Dynamic instability enables the efficient search of microtubules in space (30). Similarly, dynamic switching of bacterial cells enables bacterial populations to efficiently spread through and colonize flow networks. Dynamic switching dictates the initial stages of biofilm organization and lays the foundation for mature biofilm development.

## Results

**Spatial and Temporal Dynamics of *P. aeruginosa* Surface Attachment in Flow.** We explored the spatial organization of bacterial colonization in flow by tracking the movements of individual *P. aeruginosa* cells on surfaces in microfluidic devices (Fig. 1*A* and Movie S1). *P. aeruginosa* was initially loaded into a device, and a fraction of the population attached immediately to the cover-glass surface. Cell-free medium was flowed into the device at a constant rate to generate stable laminar flow, which was verified by using fluorescent microtracer beads. During a 30-min period, we observed multiple cell phenotypes, including the movement of cells in the upstream direction, the detachment of cells from the surface, and the reattachment of cells to the surface from a previous upstream position (marked as yellow stars in Fig. 1*A*). We observed little or no irreversibly attached cells during this period.

These observations suggest that cell movements in flow follow an ordered sequence of events. To determine the sequence, we tracked a single cell lineage over the span of six cell doublings (Fig. 1*B* and Movie S2). We observed repeated cycles in which a cell migrated on the surface and duplicated, and one cell detached from the surface while the other continued surface migration. The cell that detached from the surface was transported at high speed downstream along the streamlines of the bulk flow. The establishment of cells on the surface downstream of this area demonstrated that cells in the bulk reattached to the surface. These cells resumed upstream movement, completing the cycle of cell migration.

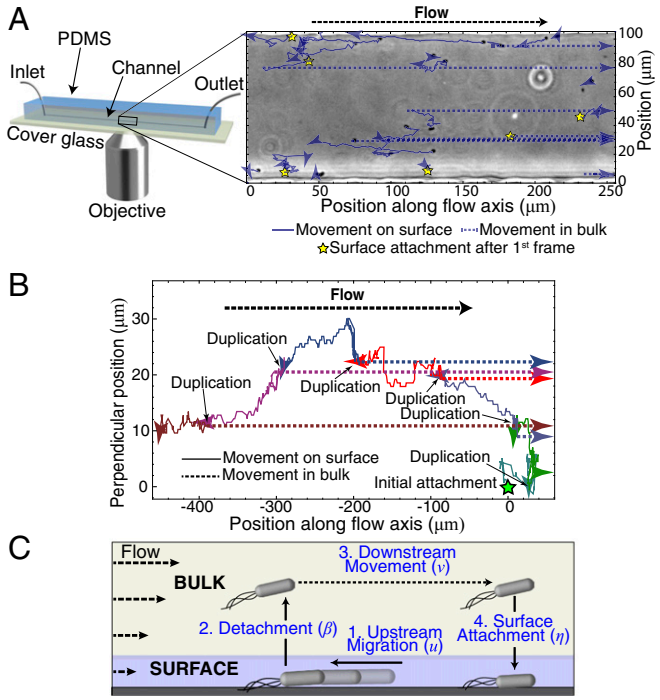


**Fig. 1.** Model of colonization under flow. (*A*) Trajectories of surface-associated *P. aeruginosa* cells in a 200 × 50 μm ($w \times h$) microfluidic device in which cell-free LB medium was flowed from left to right at 5 μL/min. Images were acquired for 30 min at 30-s intervals. Trajectories are superimposed over a phase contrast image at the start of the experiment. Cells move on surfaces (solid lines), detach from the surface, and move downstream in the bulk (dashed lines). (*B*) Trace of a single cell lineage over the course of 6 h. (*C*) Schematic summarizing the processes (blue) observed in *A* and *B*.

To quantitatively probe and understand the dynamic behaviors we observed, we developed a surface colonization model in which bacteria perform repeated cycles of: (*i*) upstream movement on the surface at an average speed $u$; (*ii*) detachment from the surface to the bulk at a rate $\beta$; (*iii*) movement downstream in the bulk at an average speed $v$; and (*iv*) reattachment from the bulk to the surface at a rate $\eta$ (Fig. 1*C*). Cells duplicate in the bulk and on surfaces at a rate $\alpha$. We describe the dynamics on the surface by the equation:

$$\partial_t \rho_s + u\partial_x \rho_s = (\alpha - \beta)\rho_s + \eta\rho_b, \quad [1]$$

where $\rho_s$ and $\rho_b$ define the bacterial population densities (number of bacteria per unit length) on the surface and in the bulk, respectively, and the upstream direction is defined toward decreasing $x$. Cells are exchanged between the surface and the bulk phases, which is described by the terms $-\beta\rho_s + \eta\rho_b$. The dynamics in the bulk are described by an equation of similar form:

$$\partial_t \rho_b + v\partial_x \rho_b = (\alpha - \eta)\rho_b + \beta\rho_s, \quad [2]$$

where exchange between the phases is described by the terms $-\eta\rho_b + \beta\rho_s$. Cells moved upstream on surfaces and downstream in the bulk, constraining the velocities to $u \leq 0$ and $v \geq 0$.

We refer to the continuous exchange of cells between two phases in flow as "dynamic switching." To determine the role of dynamic switching during biofilm development, we simulated the equations using physiological parameters. Previous measurements indicated that *P. aeruginosa* cells move upstream on surfaces at an average speed of 1 μm/min (6, 25) and move downstream in the bulk at a rate of 1,000–15,000 μm/min (*SI Appendix*). The process of attaching to and detaching from surfaces is controlled by interactions between components of type IV pili and surfaces (26, 31). We modeled this as an adsorption–desorption process in which *P. aeruginosa* cells are adsorbed to the surface and are desorbed to the bulk. Here, the attachment rate $\eta$ and the detachment rate $\beta$ are expressed as functions of a chemical potential: $\eta = A\exp(-\mu_a/k_BT)$ and $\beta = B\exp(-\mu_d/k_BT)$, where $\mu_a$ and $\mu_d$ are the chemical potentials for attaching to and detaching from surfaces, respectively; $A$ and $B$ are spatial configuration coefficients; $k_B$ is the Boltzmann constant; and $T$ is the temperature. The rates are described by $\beta = K\eta^{1/c}$, where $K$ is the spatial configuration coefficient and $c$ relates the chemical potentials: $\mu_a = c\mu_d$ (see *SI Appendix* for further details). We set the chemical potentials to be equal and opposite ($c = -1$) and the spatial configuration coefficient to 1 to reflect that attachment and detachment of *P. aeruginosa* cells from surfaces using type IV pili have not been associated with different energies or spatial configurations. This simplifies the relationship to: $\beta = 1/\eta$, where $\eta$ is a measure of surface adhesivity and $\beta$ is the inverse of this quantity. Small values of $\beta$ indicate high surface adhesivity, and, conversely, large values indicate low adhesivity.

To test our model, we compared simulated surface cell densities with those from a colonization experiment in our microfluidic device. Wild-type *P. aeruginosa* expressing GFP was flowed in from a side channel into a main channel through which cell-free LB medium was flowed (Fig. 2*A*). During 13 h of constant flow at room temperature, we observed the surface colonization established within the device, the expansion of the population in the upstream direction, and a slight decline in surface density toward the downstream direction (Fig. 2*B*). At later times, we observed a mature dense biofilm in the channel.

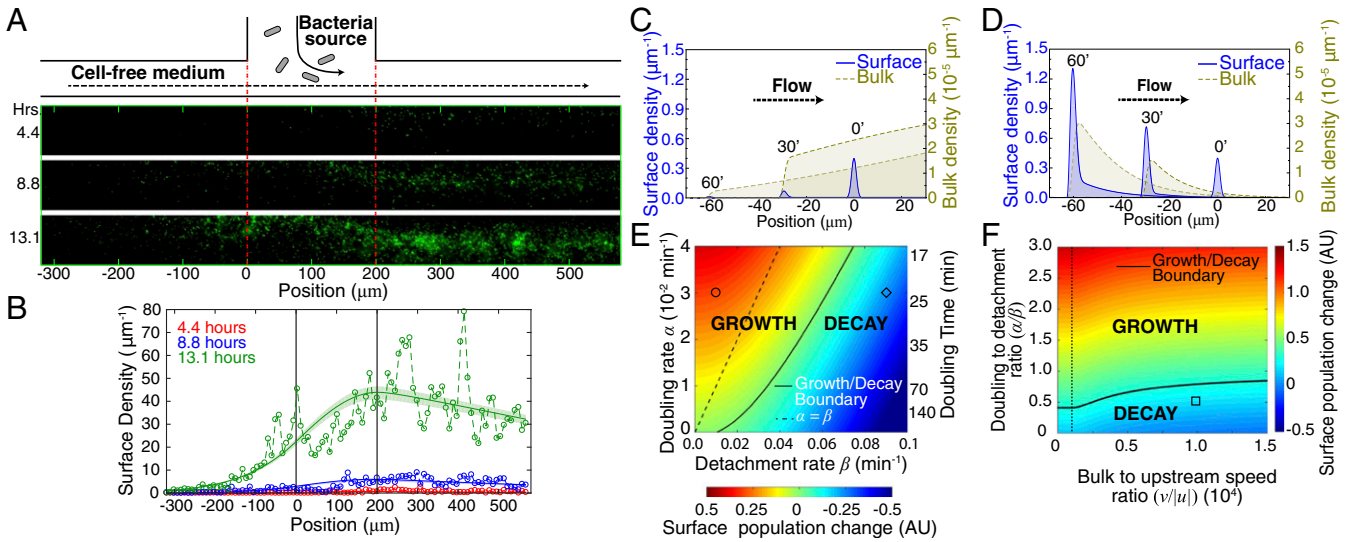


**Fig. 2.** Dynamic switching guides initial *P. aeruginosa* colonization, which exhibits only two modes in flow: growth or decay. (*A*) Schematic and corresponding fluorescence images of surface-associated *P. aeruginosa* cells that constitutively express GFP. Cells are flowed in through a side channel continuously, and cell-free LB is flowed from left to right in the main channel. (*B*) The experimental (open circles connected by dashed lines) and simulation of dynamic switching (solid lines) surface densities of *P. aeruginosa* cells after 4.4 (red), 8.8 (blue), and 13.1 (green) h of continuous flow. A continuous cell source between 0 and 200 μm and $\alpha/\beta = 0.50$ were simulated. Shaded regions indicate the 95% confidence interval for fitting the scaling parameter of the simulation to the experimental data. (*C* and *D*) Simulations show that surface colonization decays for a small ratio ($\alpha/\beta = 1/3$) (*C*) and grows for a large ratio ($\alpha/\beta = 3$) (*D*). Surface (blue) and bulk (beige) densities are plotted for 0, 30, and 60 min with a flow speed of 1 mm/min. Arrow indicates direction of flow. (*E*) Surface populations either increase (yellow–red) or decrease (blue–green) for the majority of physiological values of doubling rates ($\alpha$) and surface detachment rates ($\beta$). Steady states (solid line) are observed for a narrow range of parameters. Color bars indicate the change in surface population. The diamond and circle indicate the parameters used to generate the decay and growth profiles plotted in *C* and *D*, respectively. (*F*) Surface populations for a range of growth to detachment ($\alpha/\beta$) and upstream to downstream speed ratios. Vertical dashed line indicates the speeds used in *E*. The square indicates the values used for the simulation in *B*. See *SI Appendix* for further simulation details.

We simulated dynamic switching equations and found that these experimental surface densities were reproduced by using a doubling time of 96 min and a detachment time of 50 min per detachment, corresponding to $\alpha/\beta = 0.50$. The simulation results fit well with the experimental data for 4.4, 8.8, and 13.1 h of continuous flow, with $R$ values of 0.54, 0.76, and 0.83, respectively (Fig. 2*B* and *SI Appendix*, Fig. S2). In addition, the simulations exhibited the behaviors observed in the microfluidic channels (Fig. 2 *A* and *B*), including total population expansion, population expansion in the upstream direction, colonization in the downstream direction, and a population density profile that decreases toward the downstream direction (*SI Appendix*, Fig. S2).

The growth and detachment rates, $\alpha$ and $\beta$, respectively, were the primary parameters in our simulations. To develop an intuition for how these parameters influence surface colonization, we performed simulations with values of $\alpha/\beta$ above and below those used to fit the experimental data in Fig. 2*B*. We used values of $\alpha/\beta = 1/3$ or $\alpha/\beta = 3$, which corresponded to cells that detach from surfaces at relatively high or low rates (Fig. 2 *C* and *D* and *SI Appendix*, Fig. S1), respectively. We initially seeded the surface with a normally distributed population of bacteria centered at $x = 0$ in a linear one-dimensional flow environment and plotted the time evolution of bacterial population densities on the surface and in the bulk. The surface populations migrated upstream (toward negative $x$) with respect to time. For $\alpha/\beta = 1/3$ (a high rate of detachment), the amplitude of the surface population diminished toward extinction due to the transfer of the population from the surface to the bulk (Fig. 2*C* and *SI Appendix*, Fig. S1*A*). Cells reattached to the surface at low frequency and were swept along with the bulk. In contrast, for $\alpha/\beta = 3$ (a low rate of detachment), the shape of the surface population changed considerably, and colonization was observed both upstream and downstream of the initial seeding area (Fig. 2*D* and *SI Appendix*, Fig. S1*B*). In particular, the reattachment of cells downstream of the peak broadened the spatial distribution of bacteria along the direction of flow. Thus, the value of $\alpha/\beta$ determines whether a bacterial population on the surface expands or becomes extinct.

**Colonization Is Established by Dynamic Switching.** Bacteria encounter a variety of nutrient sources, surface chemistries, and flow rates in natural environments and infectious settings. We determined how these variables affect surface colonization for growth rates ($\alpha$) ranging from no growth to a rapid doubling time of 20 min and for a range of surface detachment rates ($\beta$) (Fig. 2 *E* and *F*). We observed surface colonization growth for low detachment rates and surface colonization decay for high detachment rates, consistent with the surface colonization plots in *Spatial and Temporal Dynamics of P. aeruginosa Surface Attachment in Flow*. Interestingly, colonization growth was possible with a continuous supply of nonproliferating cells ($\alpha = 0$ min$^{-1}$) for a small range of detachment rates ($\beta < 0.01$ min$^{-1}$) (Fig. 2*E*). We found that the vast majority of parameters resulted in only two modes of surface colonization: growth or decay (Fig. 2*E*). A steady state was only observed for a small number of parameters that formed the transition between the growth and decay modes. This result suggests that surface colonization for the majority of growth rates and surface conditions is unstable: Populations either decrease or increase on surfaces but do not remain constant. We note that our model does not account for changes relating to nutrient transport, gene regulation, and the mechanical environment that accompany the transition from low to high population densities. The population instability described here thus applies to the initial stages of colonization in which cells grow at low density.

Next, we determined how flow rates affect surface colonization near the initial seeding site. We performed simulations for bulk velocities ranging from 0 to 15 mm/min (Fig. 2*F*) for a range of the growth and surface detachment rates inclusive of those above. Again, we observed that surface population either grew or

decayed for the majority of flow rates and contained a small number of steady states at the transition between the two modes (Fig. 2*F*). Furthermore, we note that dynamic switching applies to bacteria that do not move upstream on surfaces, which corresponds to $u \geq 0$. Together, these results indicate that bacterial surface colonization in the vast majority of physiological environments, flow conditions, and bacterial species obey only two modes: growth or decay. In particular, dynamic switching controls the spatial and temporal organization of bacterial colonization in flow.

We note that the values used to compare the simulations with the microfluidic data (Fig. 2*B*) were $\alpha/\beta = 0.50$ and $v/|u| = 10{,}000$, which dictated that the population should decay weakly near the steady state (Fig. 2*F*), while the experimental and simulation results indicated that the populations grow. This effect is due to the addition of a continuous cell source, which increases the effective growth rate and results in overall population growth. Thus, our simulation of dynamic switching is in agreement with all of the behaviors observed during colonization of *P. aeruginosa* in flow in the microfluidic devices.

**Simulating Colonization in Vasculature.** Bacterial colonization is a critical step for causing infection and disease in plants and animals. We explored the role of dynamic switching in establishing bacterial colonization in plant and animal vascular flow networks. Vascular networks in these organisms contain complex geometries and topologies that give rise to a large number of flow bifurcations and branches (32, 33). The colonization of vasculature is observed in many types of animal and plant infections. However, there is no theoretical or computational framework that describes the dispersal and growth of bacteria in these flow networks. We attribute the lack of this framework to a lack of an accurate model describing bacterial colonization in flow.

Using our dynamic switching model, we simulated bacterial colonization in vasculature in silico for a branched channel in which fluid moves from left to right and bifurcates into two separate branches (Fig. 3*A*). We extended Eqs. **1** and **2**, which encode the surface and bulk population densities for a single branch, to two linear branches and included an additional term that enabled the exchange of cells between the two branches upstream of the bifurcation (Fig. 3*A* and see *SI Appendix* for details). We initially seeded *P. aeruginosa* in the top branch to simulate an infection condition (Fig. 3*A*) and determined the time evolution of the cell population densities using parameters that establish surface population growth ($\alpha/\beta = 0.7$). Our results indicated that surface colonization evolves in the branched channel through a specific sequence of events: (*i*) upstream population expansion from the seeded branch, (*ii*) movement across flow streamlines, and (*iii*) downstream dispersal to the side branch (Fig. 3*B* and *SI Appendix*, Fig. S3*A*). Dynamic switching occurred throughout the entire process, with cells continually detaching from surfaces, moving downstream with the bulk, and reattaching at a downstream position (Fig. 3*B* and *SI Appendix*, Fig. S3*A*). Our model thus predicts that colonization expands upstream and spreads downstream to neighboring branches.

We compared our results with a colonization experiment in a branched microfluidic device. Consistent with our simulation conditions, cell-free medium was flowed through a main branch and diverges into two separate branches. We inoculated one branch (the seeded branch) with coculture containing wild-type *P. aeruginosa* expressing GFP and a Δ*pilTU* mutant (expressing mCherry) that is unable to move upstream, which served as a reference for the initial inoculation site. During 15 h of constant flow, we observed spatial and temporal population changes in the identical sequence as our dynamic switching model: Wild-type *P. aeruginosa* moved upstream, across streamlines, and downstream in the side branch (Fig. 3*C* and *SI Appendix*, Fig. S3*B*). We observed agreement of the experimental and simulated surface densities, with $R$ values of 0.86 and 0.68 in the seeded and side branches, respectively (Fig. 3*D* and *SI Appendix*, Fig. S3*C*). Our dynamic switching model thus recapitulates bacterial colonization in a simple flow network.

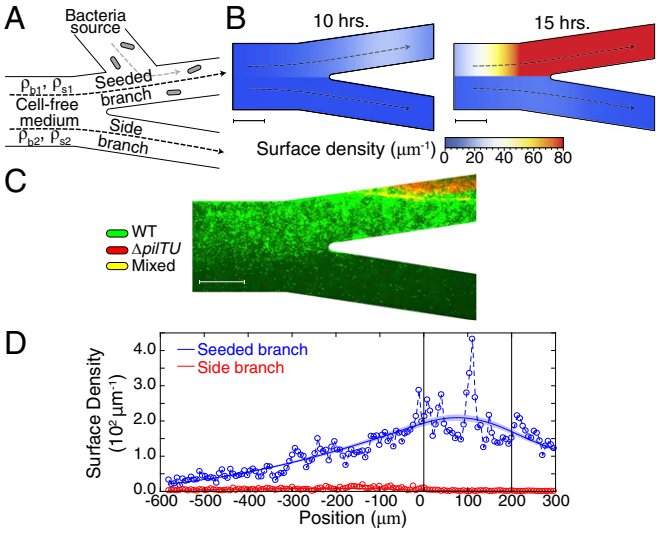


**Fig. 3.** Dynamic switching determines the dynamics of *P. aeruginosa* colonization in branched flow networks. (*A*) Schematic of a branched environment in which bacteria and cell-free medium are continuously flowed through the side and main channels, respectively. The functions $\rho_s$ and $\rho_b$ represent the surface and bulk densities, respectively, in each branch. (*B*) Surface densities in a simulation of dynamic switching in a branched environment. Dashed lines with arrows indicate the bulk flow from left to right, and color bars indicate the surface cell density. Plots were generated by using $\alpha/\beta = 0.7$ for 10 and 15 h of continuous flow in which cells were seeded continuously at a position 20 μm downstream of the branch intersection using an inlet width of 200 μm. (*C*) Fluorescence image of surface colonization in a branched microfluidic device in which wild-type (green) and Δ*pilTU* (red) *P. aeruginosa* and cell-free medium were flowed continuously through the seeded and main branches, respectively, for 15 h. (*D*) The experimental (open circles connected by dashed lines) and simulated (solid lines) surface densities in the seeded (blue) and side (red) branches at 15 h. Shaded regions indicate the 95% confidence interval for fitting the scaling parameter of the simulation to the experimental data. (Scale bars, 50 μm.) See *SI Appendix* for further simulation details.

To test the ability of our model and framework to predict colonization in generalized flow networks, we simulated a network with increased complexity in which a main branch bifurcated at nodes separated by different distances into four branches (Fig. 4*A*). We seeded cells in an initial branch and simulated the time evolution of colonization (Fig. 4*B* and *SI Appendix*, Fig. S4) using parameters that corresponded to the colonization growth mode ($v/|u| = 1{,}000$ and $\alpha/\beta = 0.67$). We observed colonization upstream of the seeded branch (branch 1) and dispersal to neighboring branches in succession from branches 1 to 4. The upstream movement on surfaces enabled cells to reach an upstream node. The subsequent transverse cellular movements enabled cells to enter the streamlines of a neighboring branch, where they rapidly moved downstream via the bulk. These results suggest a general strategy for bacterial dispersal in vasculature: Cells move upstream slowly on surfaces, move transversely into adjacent branches at junctions, and move into the bulk. This results in the dispersal of cells downstream at speeds that are many orders of magnitude higher than on surfaces.

**Dynamic Switching Enables Efficient Dispersal.** To quantify the extent to which dynamic switching affects bacterial dispersal in flow networks, we ran our simulation in the generalized four-branch flow system (Fig. 4 *A* and *B* and *SI Appendix*, Fig. S4) and determined the extent of flow network coverage for surface detachment rates corresponding to surface-dominated lifestyles, dynamic switching,

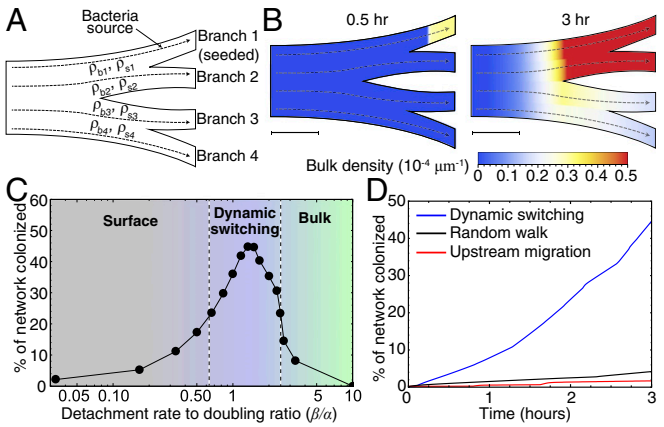


**Fig. 4.** Dynamic switching increases bacterial dispersal in flow networks. (*A* and *B*) Schematic (*A*) and simulation (*B*) of bacterial dispersal in a generalized flow network containing four branches. Branch 1 is initially seeded with bacteria. The bulk cell density is shown. Cells disperse to neighboring branches by moving upstream on surfaces and downstream in the bulk. Dashed lines with arrows indicate the bulk flow from left to right, and color bars indicate bulk cell densities. Plots were generated by using $\beta/\alpha = 1.5$. (Scale bars, 50 μm.) (*C*) Flow network surface colonization for surface-dominated, dynamic switching, and bulk-dominated modes of motility in a four-branch flow network. The plot shows the proportion of the network that is surface-colonized at 3 h of simulated time using $\alpha = 0.03$ min$^{-1}$ and a range of detachment rates ($\beta$). The coverage is maximum at $\beta/\alpha = 1.5$. The vertical dashed lines indicate the values of $\beta/\alpha$ for which the coverage is half-maximum. (*D*) Network surface colonization for dynamic switching, random walk, and upstream surface-only motility models. Cells in the random walk and upstream models are constrained to the surface and do not exchange with the bulk. Plots were generated by using $\beta/\alpha = 1.5$ for dynamic switching, $D = 1$ μm$^2$/min for the random walk, and speed of $u = 1$ μm/min for upstream surface-only motility.

and bulk-dominated lifestyles. For surface- or bulk-dominated lifestyles, cells generally remained in their respective phases, and the cell exchange between the two phases was low (Fig. 4*C*). For the dynamic switching regime, cells transferred continuously between the surface and bulk phases. We observed low network dispersal for surface- and bulk-dominated lifestyles (Fig. 4*C* and *SI Appendix*, Fig. S5). In contrast, dynamic switching significantly increased the network coverage, with maximum network coverage observed at $\beta/\alpha = 1.5$ and the half-maximum range observed at $\beta/\alpha$ values between 0.7 and 2.4 (Fig. 4*C*). The dispersal effects of dynamic switching were striking when network coverage was compared against surface-only motility, in which cells explored networks using random walks ($D = 1$ μm$^2$/min) or upstream migration (Fig. 4*D*). In particular, our results show that dynamic switching enables rapid dispersal throughout the flow network whereas surface-only motility results in relatively slow dispersal. The effect of dynamic switching on dispersal is independent of the number of branches and is observed in single- and two-branch networks as well (*SI Appendix*, Fig. S6), which suggests that the effects of dynamic switching are independent of flow network geometry. Together, these results show that dynamic switching by bacteria provides significant dispersal and colonization advantages over surface- and bulk-only modes. In particular, the movement between two phases (bulk and surface) maximizes dispersal, whereas movement constrained to a single phase significantly limits dispersal.

## Discussion

**Efficient Exploration of Space by Dynamic Switching.** The efficient exploration of space is a ubiquitous theme in biological systems. For example, microtubules search intracellular space to capture chromosomes during cell division, and transcription factors search chromosomal positions to bind target sites to regulate gene expression. In natural and infection settings, bacteria search through fluidic spaces to colonize environments that are favorable for their survival, such as those that are nutrient-rich, free of competing bacterial species, and secluded from host defenses. Our results show that *P. aeruginosa* uses dynamic switching, a strategy consisting of continuous switching between surfaces and the bulk, to disperse throughout and colonize environments.

The equations that describe dynamic switching (Eqs. **1** and **2**) have an identical form to those that describe the dynamic instability of microtubules (29). The equations for dynamic instability encode two states of microtubule polymerization (growth and decay), whereas those for dynamic switching encode two modalities of bacterial dispersal (on surfaces and in the bulk). The continuous switching between two states enables microtubules to search for space efficiently for the capture of chromosomes (30). Our work demonstrates that dynamic switching between two modalities by *P. aeruginosa* significantly increases the efficiency by which cells disperse throughout and colonize flow networks such as those found in host blood and lung vasculature (Fig. 4*B* and *SI Appendix*, Fig. S4). Dynamic switching is thus likely to play a significant role in host pathogenesis by facilitating the transport and colonization of pathogens to infection sites. In particular, our current simulations (Figs. 3 and 4) are well suited to describe the entry, dispersal, and colonization of bacteria near a wound site in a vascular network. Our simulations show that bacterial colonization is maximized in conditions that enable dynamic switching and is significantly diminished for single-state lifestyles in which cells either adhere strongly to surfaces or do not adhere to them at all (Fig. 4*C* and *SI Appendix*, Fig. S5). Dynamic switching thus requires intermediate values of surface adhesivity (i.e., $0.7 < \beta/\alpha < 2.4$ in Fig. 4*C*) to facilitate both surface adhesion and release. We observed that *P. aeruginosa* colonization in our microfluidic experiments corresponded to $\beta/\alpha$ values of 2.0 and 1.4 in the single and two-branch geometries, respectively (Figs. 2*B* and 3*D*). These results suggest that *P. aeruginosa* and other pathogens that utilize dynamic switching have evolved surface attachment mechanisms that result in intermediate surface adhesivity. In particular, the hypermutability of pilus and other adhesion components (34–36) could facilitate cellular adaptation to different surfaces in natural and infection settings, thereby tuning the extent of dynamic switching.

**Dynamic Switching Dictates Initial Biofilm Organization in Flow.** Surface attachment is a requirement for biofilm formation (2, 17–19). Our results suggest that dynamic switching plays a critical role in the spatial organization of biofilms by determining the initial distribution of bacteria on surfaces. Dynamic switching increases the spatial distribution of biofilm initiation sites by maximizing surface colonization along all portions of the network (Fig. 4*C*). In addition, our simulations show that initial surface populations either grow or decay for the majority of surface adhesivity and nutrient availability conditions and are fixed for a small number of conditions (Fig. 2 *E* and *F*). After initial surface attachment, biofilm development adds additional layers of cells that provide insulation from the effects of flow. Nutrient absorption, cell attachment, and cell detachment significantly decrease within the interior of the biofilm, terminating dynamic switching. According to our model (Eqs. **1** and **2**), this allows for the possibility of population stability (Fig. 2*E*). Thus, the transition from dynamic switching to mature biofilm formation enables populations to change from a state in which populations are either growing or decaying to a state that permits the establishment of stable communities. Due to the insular nature of biofilms, these communities may enable survival and dispersal over a larger area and in conditions that would be prohibitive for individual cells. Future work will need to address the effects of flow, nutrient transport, and bacterial cell exchange during this critical transition.

Dynamic switching is likely to play an important role in shaping the spatial organization of polymicrobial environments,

in which different microbes compete for limited nutrients. Future work will need to incorporate the effects of dynamic switching in environments containing multiple species and host network geometries. In particular, the equations that describe dynamic switching apply generally to biphasic populations and are not limited to bacteria that move upstream on surfaces or adhere strongly to surfaces. Upstream-deficient bacteria can be represented by $u = 0$ in our model, and bacteria that do not adhere strongly are represented by large values of $\beta$. Furthermore, the framework developed here can be expanded to accommodate multiple species and arbitrary flow network geometries by solving systems of one-dimensional equations. Thus, the framework developed here can be applied to predict the dispersal and colonization dynamics of *P. aeruginosa* and other bacteria in complex flow networks such as those found in hosts.

**Dynamic Switching: Potential Role as a General Dispersal Mechanism.** At the most fundamental level, dynamic switching describes individual cells that repeatedly transition between surface attachment and advection in a moving bulk. This behavior is not limited to bacteria. We speculate that dynamic switching could have a role in cellular processes that generally increase spatial distribution. For example, leukocytes are trafficked in two phases by circulation in the bloodstream and recruitment to surfaces (37, 38). The exchange of leukocytes between the two phases could enable effective dispersal throughout the body, which is critical for effective tissue repair. Similarly, dynamic switching could have a role in the spread of metastatic cancers, which involves the movement of tumor cells on surfaces and in the bulk of circulatory networks (39, 40). Given these potential roles, interfering with dynamic switching mechanisms may represent a potential strategy for the treatment of bacterial infections and other diseases.

## Experimental Procedures

Bacterial strains were grown in LB-Miller (BD Difco) broth overnight to saturation, diluted 1:1,000, and regrown in the same medium to midexponential phase. Microfluidic devices were fabricated by using soft photolithography as described (6). The dynamic switching equations (Eqs. **1** and **2**) were encoded in Matlab (Version R2015a; MathWorks) by using the finite-difference method, a second-order upwind scheme, and Neumann boundary conditions. Details on bacterial strains, growth conditions, microfluidic experiments, simulation parameters, and the model can be found in *SI Appendix*.

**ACKNOWLEDGMENTS.** We thank J. Allard and J. Newby for insight into the Dogterom-Leibler model; Z. Gitai for helpful discussions and comments on the manuscript; and J. Shaevitz, N. Wingreen, and the University of California, Irvine Systems Microbiology group for helpful discussions. This work was supported by National Science Foundation Grant 1330288 (to H.A.S.) and National Institutes of Health Career Transition Award K22AI112816 (to A.S.).

1. Hall-Stoodley L, Costerton JW, Stoodley P (2004) Bacterial biofilms: From the natural environment to infectious diseases. *Nat Rev Microbiol* 2:95–108.
2. López D, Vlamakis H, Kolter R (2010) Biofilms. *Cold Spring Harb Perspect Biol* 2: a000398.
3. Danhorn T, Fuqua C (2007) Biofilm formation by plant-associated bacteria. *Annu Rev Microbiol* 61:401–422.
4. Nadell CD, Xavier JB, Foster KR (2009) The sociobiology of biofilms. *FEMS Microbiol Rev* 33:206–224.
5. Asally M, et al. (2012) Localized cell death focuses mechanical forces during 3D patterning in a biofilm. *Proc Natl Acad Sci USA* 109:18891–18896.
6. Siryaporn A, Kim MK, Shen Y, Stone HA, Gitai Z (2015) Colonization, competition, and dispersal of pathogens in fluid flow networks. *Curr Biol* 25:1201–1207.
7. Persat A, Stone HA, Gitai Z (2014) The curved shape of *Caulobacter crescentus* enhances surface colonization in flow. *Nat Commun* 5:3824.
8. Drescher K, et al. (2016) Architectural transitions in *Vibrio cholerae* biofilms at single-cell resolution. *Proc Natl Acad Sci USA* 113:E2066–E2072.
9. Yan J, Sharo AG, Stone HA, Wingreen NS, Bassler BL (2016) *Vibrio cholerae* biofilm growth program and architecture revealed by single-cell live imaging. *Proc Natl Acad Sci USA* 113:E5337–E5343.
10. Spiers AJ, Bohannon J, Gehrig SM, Rainey PB (2003) Biofilm formation at the air-liquid interface by the *Pseudomonas fluorescens* SBW25 wrinkly spreader requires an acetylated form of cellulose. *Mol Microbiol* 50:15–27.
11. Dietrich LEP, et al. (2013) Bacterial community morphogenesis is intimately linked to the intracellular redox state. *J Bacteriol* 195:1371–1380.
12. Rusconi R, Lecuyer S, Guglielmini L, Stone HA (2010) Laminar flow around corners triggers the formation of biofilm streamers. *J R Soc Interface* 7:1293–1299.
13. Drescher K, Shen Y, Bassler BL, Stone HA (2013) Biofilm streamers cause catastrophic disruption of flow with consequences for environmental and medical systems. *Proc Natl Acad Sci USA* 110:4345–4350.
14. Kim MK, Drescher K, Pak OS, Bassler BL, Stone HA (2014) Filaments in curved streamlines: Rapid formation of *Staphylococcus aureus* biofilm streamers. *New J Phys* 16:065024.
15. Persat A, et al. (2015) The mechanical world of bacteria. *Cell* 161:988–997.
16. Yawata Y, Nguyen J, Stocker R, Rusconi R (2016) Microfluidic studies of biofilm formation in dynamic environments. *J Bacteriol* 198:2589–2595.
17. Monds RD, O'Toole GA (2009) The developmental model of microbial biofilms: Ten years of a paradigm up for review. *Trends Microbiol* 17:73–87.
18. O'Toole GA, Kolter R (1998) Flagellar and twitching motility are necessary for *Pseudomonas aeruginosa* biofilm development. *Mol Microbiol* 30:295–304.
19. O'Toole GA, Kolter R (1998) Initiation of biofilm formation in *Pseudomonas fluorescens* WCS365 proceeds via multiple, convergent signalling pathways: A genetic analysis. *Mol Microbiol* 28:449–461.
20. Siryaporn A, Kuchma SL, O'Toole GA, Gitai Z (2014) Surface attachment induces *Pseudomonas aeruginosa* virulence. *Proc Natl Acad Sci USA* 111:16860–16865.
21. Islam MS, Krachler AM (2016) Mechanosensing regulates virulence in *Escherichia coli* O157:H7. *Gut Microbes* 7:63–67.
22. Persat A, Inclan YF, Engel JN, Stone HA, Gitai Z (2015) Type IV pili mechanochemically regulate virulence factors in *Pseudomonas aeruginosa*. *Proc Natl Acad Sci USA* 112: 7563–7568.
23. Korber DR, Lawrence JR, Caldwell DE (1994) Effect of motility on surface colonization and reproductive success of *Pseudomonas fluorescens* in dual-dilution continuous culture and batch culture systems. *Appl Environ Microbiol* 60:1421–1429.
24. Dogterom M, Leibler S (1993) Physical aspects of the growth and regulation of microtubule structures. *Phys Rev Lett* 70:1347–1350.
25. Holy TE, Leibler S (1994) Dynamic instability of microtubules as an efficient way to search in space. *Proc Natl Acad Sci USA* 91:5682–5685.
26. Meng Y, et al. (2005) Upstream migration of *Xylella fastidiosa* via pilus-driven twitching motility. *J Bacteriol* 187:5560–5567.
27. Shen Y, Siryaporn A, Lecuyer S, Gitai Z, Stone HA (2012) Flow directs surface-attached bacteria to twitch upstream. *Biophys J* 103:146–151.
28. Mattick JS, Type IV (2002) Type IV pili and twitching motility. *Annu Rev Microbiol* 56: 289–314.
29. Vallet I, et al. (2004) Biofilm formation in *Pseudomonas aeruginosa*: Fimbrial cup gene clusters are controlled by the transcriptional regulator MvaT. *J Bacteriol* 186: 2880–2890.
30. Vallet I, Olson JW, Lory S, Lazdunski A, Filloux A (2001) The chaperone/usher pathways of *Pseudomonas aeruginosa*: Identification of fimbrial gene clusters (cup) and their involvement in biofilm formation. *Proc Natl Acad Sci USA* 98:6911–6916.
31. Klausen M, et al. (2003) Biofilm formation by *Pseudomonas aeruginosa* wild type, flagella and type IV pili mutants. *Mol Microbiol* 48:1511–1524.
32. Bohn S, Andreotti B, Douady S, Munzinger J, Couder Y (2002) Constitutive property of the local organization of leaf venation networks. *Phys Rev E Stat Nonlin Soft Matter Phys* 65:061914.
33. West GB, Brown JH, Enquist BJ (1999) The fourth dimension of life: Fractal geometry and allometric scaling of organisms. *Science* 284:1677–1679.
34. Abraham JM, Freitag CS, Clements JR, Eisenstein BI (1985) An invertible element of DNA controls phase variation of type 1 fimbriae of *Escherichia coli*. *Proc Natl Acad Sci USA* 82:5724–5727.
35. Marrs CF, Ruehl WW, Schoolnik GK, Falkow S (1988) Pilin-gene phase variation of *Moraxella bovis* is caused by an inversion of the pilin genes. *J Bacteriol* 170: 3032–3039.
36. Willems R, Paul A, van der Heide HG, ter Avest AR, Mooi FR (1990) Fimbrial phase variation in *Bordetella pertussis*: A novel mechanism for transcriptional regulation. *EMBO J* 9:2803–2809.
37. Shi C, Pamer EG (2011) Monocyte recruitment during infection and inflammation. *Nat Rev Immunol* 11:762–774.
38. Ley K (1996) Molecular mechanisms of leukocyte recruitment in the inflammatory process. *Cardiovasc Res* 32:733–742.
39. Geng Y, Marshall JR, King MR (2012) Glycomechanics of the metastatic cascade: Tumor cell-endothelial cell interactions in the circulation. *Ann Biomed Eng* 40:790–805.
40. Takeishi N, Imai Y, Yamaguchi T, Ishikawa T (2015) Flow of a circulating tumor cell and red blood cells in microvessels. *Phys Rev E Stat Nonlin Soft Matter Phys* 92:063011.